A tetrahedral entropy for water

Pradeep Kumar[a,1], Sergey V. Buldyrev[b], and H. Eugene Stanley[c,1]

[a]Center for Studies in Physics and Biology, The Rockefeller University, 1230 York Avenue, New York, NY 10021; [b]Department of Physics, Yeshiva University, 500 West 185th Street, New York, NY 10033; and [c]Center for Polymer Studies and Department of Physics, Boston University, Boston, MA 02215

Contributed by H. Eugene Stanley, October 5, 2009 (sent for review May 15, 2009)

We introduce the space-dependent correlation function $C_Q(r)$ and time-dependent autocorrelation function $C_Q(t)$ of the local tetrahedral order parameter $Q \equiv Q(r,t)$. By using computer simulations of 512 waterlike particles interacting through the transferable interaction potential with five points (TIP5 potential), we investigate $C_Q(r)$ in a broad region of the phase diagram. We find that at low temperatures $C_Q(t)$ exhibits a two-step time-dependent decay similar to the self-intermediate scattering function and that the corresponding correlation time τ_Q displays a dynamic cross-over from non-Arrhenius behavior for $T > T_W$ to Arrhenius behavior for $T < T_W$, where T_W denotes the Widom temperature where the correlation length has a maximum as T is decreased along a constant-pressure path. We define a tetrahedral entropy S_Q associated with the local tetrahedral order of water molecules and find that it produces a major contribution to the specific heat maximum at the Widom line. Finally, we show that τ_Q can be extracted from S_Q by using an analog of the Adam–Gibbs relation.

specific heat of water | orientational entropy of tetrahedral liquids | anomalies of liquid water | Widom line

It has long been appreciated that the local structure around a molecule of liquid water arising from the vertices formed by four nearest neighbors is approximately tetrahedral at ambient pressure and that the degree of tetrahedrality increases when water is cooled (1–5). An important advance occurred in the past 10 years when computer simulations allowed the quantification of the degree of tetrahedrality (6–10) by assigning to each molecule a local tetrahedral order parameter Q (11–16). At high temperatures, the probability distribution $P(Q,T)$ is bimodal, with one peak corresponding to a high degree of tetrahedrality and the other to a less tetrahedral environment (Fig. 1). Upon decreasing temperature, the peak associated with a high degree of tetrahedrality grows, suggesting that the local structure of water becomes much more tetrahedral at lower temperatures (13, 14, 17).

Introduction

Water has been hypothesized to belong to the class of polymorphic liquids, phase separating—at sufficiently low temperatures and high pressures—into two distinct liquid phases: a high density liquid (HDL) with smaller Q and a low density liquid (LDL) with larger Q (18). The coexistence line separating these two phases may terminate at a liquid–liquid (LL) critical point, above which (in the LL supercritical region) appears a line of correlation length maximum in the pressure–temperature plane. The locus of maximum correlation length in the one-phase region is called the Widom line $T_W \equiv T_W(P)$ (19), near which different response functions, such as isobaric specific heat C_P and isothermal compressibility K_T, display maxima. Recent neutron-scattering experiments (20) and computer simulations (19) show that the dynamics of water gradually cross over from being non-Arrhenius for $T > T_W$ to Arrhenius for $T < T_W$.

Although dynamic heterogeneities have received considerable attention (21, 22), static heterogeneities have attracted less interest. In this paper, we ask how the tetrahedral order and its spatiotemporal correlations change upon crossing the Widom line. To this end, we introduce three quantities of physical interest: (*i*) the space-dependent correlation function $C_Q(r)$, (*ii*) the time-dependent autocorrelation function $C_Q(t)$, and (*iii*) the tetrahedral entropy S_Q. These functions can also be usefully applied to study other locally tetrahedral liquids, such as silicon (23–25), silica (26), and phosphorus (27).

Model

We perform molecular dynamics (MD) simulations of $N = 512$ water-like molecules interacting via the transferable interaction potential with five points (TIP5 potential), (28), which exhibits a LL critical point at $T_C \approx 217$ K and $P_C \approx 340$ MPa (29, 30). We carry out simulations in the *NPT* ensemble at atmospheric pressure ($P = 1$ atm) for temperatures ranging from 320 K down to 230 K.

Results

Space- and Time-Dependent Correlations of the Tetrahedral Order Parameter. To quantify the local degree of tetrahedrality, we calculate the local tetrahedral order parameter (13)

$$Q_k \equiv 1 - \frac{3}{8}\sum_{i}^{3}\sum_{j=i+1}^{4}\left[\cos\psi_{ikj} + \frac{1}{3}\right]^2, \qquad [1]$$

where ψ_{ikj} is the angle formed by the molecule k and its nearest neighbors i and j. The average value $\langle Q\rangle \equiv (1/N)\sum_k Q_k$ increases with decreasing T and saturates at lower T, whereas $|d\langle Q\rangle/dT|$ has a maximum at the Widom line $T_W \approx 250$ K (31–33).

To characterize the space-dependent correlations of the local order parameter, we find all the pairs of molecules i and j whose oxygens are separated by distances belonging to the interval $[r - \Delta r/2, r + \Delta r/2]$. The number of such pairs is

$$N(r,\Delta r) = \sum_{ij}\delta(r_{ij} - r, \Delta r), \qquad [2]$$

where r_{ij} is the distance between the oxygens of molecules i and j. The sum is taken over all molecules in the system and

$$\delta(r_{ij} - r, \Delta r) = \begin{cases} 1 & \text{if } |r - r_{ij}| < \Delta r/2, \\ 0 & \text{otherwise.} \end{cases} \qquad [3]$$

For $\Delta r \to 0$, $\delta(r_{ij} - r, \Delta r) \to \delta(r_{ij} - r)\Delta r$ where $\delta(r_{ij} - r)$ is the Dirac δ-function. $N(r,\Delta r)$ can be approximated as

$$N(r,\Delta r) = 4\pi r^2 N g_{OO}(r)\rho\Delta r, \qquad [4]$$

where N is the total number of molecules in the system, $g_{OO}(r)$ is the oxygen–oxygen-pair correlation function, and ρ is the number density.

Next, we find the local order parameters Q_k and Q_l for all such pairs of molecules and compute their mean,

$$Q(r) \equiv \langle Q\rangle_r \equiv \frac{\sum_{kl} Q_k \delta(r_{kl} - r, \Delta r)}{N(r_{kl} - r, \Delta r)}, \qquad [5]$$

Author contributions: P.K., S.V.B., and H.E.S. designed research, performed research, contributed new reagents/analytic tools, analyzed data, and wrote the paper.

The authors declare no conflict of interest.

Freely available online through the PNAS open access option.

[1]To whom correspondence should be addressed. E-mail: pradeep.kumar@rockefeller.edu or hes@bu.edu.

www.pnas.org/cgi/doi/10.1073/pnas.0911094106

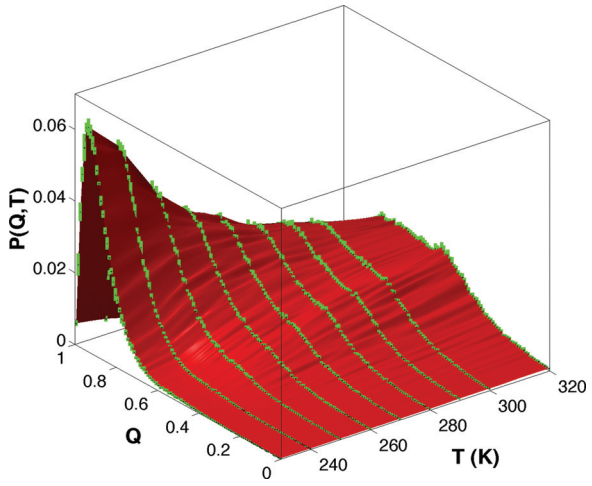

Fig. 1. Dependence on Q of the probability density function $P(Q, T)$ for nine values of T. At high T, $P(Q, T)$ is bimodal with peaks at high and low values of Q. The magnitude of the high Q value peak grows as it shifts toward the larger values of Q upon decreasing temperature whereas the magnitude of the low Q value peak decreases and, at sufficiently low temperatures, $P(Q, T)$ becomes unimodal. Analogous plots are shown for TIP4P and TIP5P models, respectively, in refs. 13 and 17. Error bars are shown in green.

their variance,

$$\sigma_Q^2(r) \equiv \langle Q^2\rangle_r - \langle Q\rangle_r^2 \equiv \sum_{kl} \frac{Q_k^2 \delta(r_{kl} - r, \Delta r)}{N(r_{kl} - r, \Delta r)} - \langle Q\rangle_r^2, \qquad [6]$$

and covariance,

$$\langle Q(r)Q(0)\rangle_r \equiv \sum_{kl} \frac{Q_k Q_l \delta(r_{kl} - r, \Delta r)}{N(r_{kl} - r, \Delta r)}. \qquad [7]$$

Finally, we introduce the space-dependent correlation function of the local tetrahedrality Q,

$$C_Q(r) \equiv \frac{\langle Q_k Q_l\rangle_r - \langle Q\rangle_r \langle Q\rangle_r}{\sigma_Q^2(r)}. \qquad [8]$$

In Figs. 2*A* and 2*B*, we show $Q(r)$ and $\sigma_Q^2(r)$ for different temperatures and atmospheric pressures. The behavior of $Q(r)$ and its variance $\sigma_Q^2(r)$ as a function of the distance r has a clear physical meaning. For molecules separated by 0.32 nm, $Q(r)$ has a deep minimum characterizing the distortion of the first tetrahedral coordination shell of the four nearest neighbors by the intrusion of a "fifth neighbor" (34). Conversely, the quantity $\sigma_Q^2(r = 0.32\text{nm}) - \sigma_Q^2(\infty)$ for such molecules dramatically increases upon decreasing temperature (see Fig. 2*C*), and has a maximum at $T \approx 246$ K, which is approximately equal to the ambient pressure value of T_W (≈ 250 K for the TIP5P model) reported in refs. 19 and 31–33. A measure qualitatively similar to $Q(r)$ has been studied in case of solvation structure of water around carbohydrate molecules (35). In Fig. 2*D*, we show $C_Q(r)$ for different temperatures for $P = 1$ atm. $C_Q(r)$ has positive maxima at positions of the first and second peaks in the oxygen–oxygen pair correlation function. Water molecules separated by $r \approx 0.32$ nm exhibit weak anticorrelation in local tetrahedral order at high temperatures, which changes to positive correlation upon decreasing the temperature below T_W.

To study the time development of the local tetrahedral order parameter, we introduce the time-dependent autocorrelation function

$$C_Q(t) \equiv \frac{\langle Q_i(t)Q_i(0)\rangle - \langle Q\rangle^2}{\langle Q^2\rangle - \langle Q_i\rangle^2}, \qquad [9]$$

where $Q_i(t)$ is the tetrahedral order parameter of each molecule in the system and $\langle Q_i\rangle$ is the ensemble average. In Fig. 3*A* we show $C_Q(t)$ for different temperatures. The decay of $C_Q(t)$ is reminiscent of the decay of the self-intermediate scattering function. The long-time behavior of $C_Q(t)$ is exponential at high T but at low T can be fit with a stretched exponential $\exp[-(t/\tau)^\beta]$, where $0 < \beta < 1$ (36).

For simplicity, we define the correlation time τ_Q as the time required for $C_Q(t)$ to decay by a factor e. Fig. 3*B* shows the values of τ_Q as function of $1/T$ on an Arrhenius plot. The behavior of τ_Q is non-Arrehenius at high temperatures and can be fit by a power law $B(T - T_{\text{MCT}})^{-\gamma}$ where $B = 25.39$, the mode coupling temperature (37) $T_{\text{MCT}} \approx 246.186$, and $\gamma = 1.17722$ are the fitting parameters. At low T, τ_Q deviates from the power-law fit and becomes Arrhenius. This cross-over in relaxation of local tetrahedral order occurs near T_W, similar to the cross-over found in density relaxation (19, 20, 38).

Tetrahedral Entropy and Tetrahedral Specific Heat. Because Q measures the local tetrahedral order, it must contribute to the entropy of the system. We next derive an expression for this "tetrahedral entropy" $S(Q_1, Q_2, \ldots, Q_N)$, which we define to be the logarithm of the number of states corresponding to the interval between $(Q_1, Q_2, \ldots, Q_N)$ and $(Q_1+\Delta Q_1, Q_2+\Delta Q_2, \ldots, Q_N+\Delta Q_N)$ in the hypercubic space formed by Qs. According to Eq. **1**, $\frac{8}{3}(1 - Q_k) = const$ defines a surface of a six-dimensional hypersphere of radius $\sqrt{\frac{8}{3}(1 - Q_k)}$ in the space defined by the cosines of the six tetrahedral angles ψ_{ikj} of Eq. **1**. Hence we assume that the number of states between Q_k and $Q_k + \Delta Q_k$ of molecule k scales as

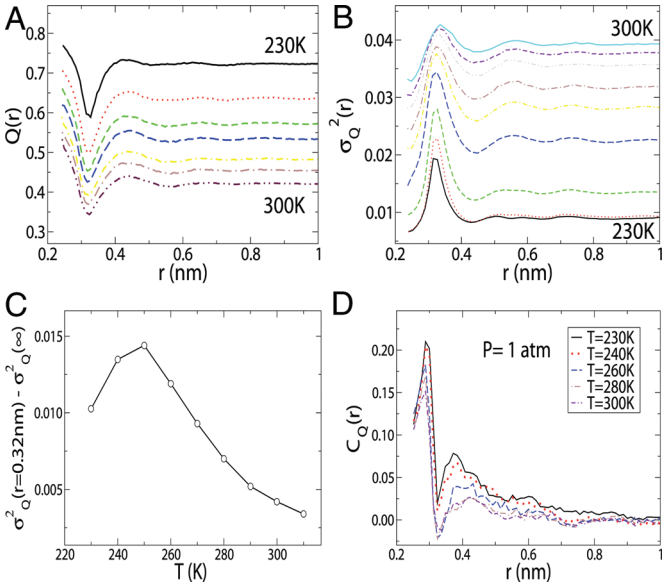

Fig. 2. Average tetrahedral order parameter, its variance and spatial correlations as functions of separation between water molecules for different temperatures. (*A* and *B*) The average order parameter $Q(r)$ (*A*) and its variance, $\sigma_Q^2(r)$ (*B*), as a function of the distance r. (*C*) Temperature dependence of $\sigma_Q^2(r = 0.32\text{nm}) - \sigma_Q^2(\infty)$ shows a maximum at the Widom temperature, suggesting that the local fluctuations in Q at the fifth-neighbor distance increase upon decreasing temperature and have a maximum at the Widom line. (*D*) Spatial correlation function $C_Q(r)$ of the tetrahedral order parameter Q (Eq. **1**) at various temperatures for pressure $P = 1$ atm. $C_Q(r)$ has positive peaks at the positions of the nearest-neighbor peaks in oxygen–oxygen pair correlation function $g_{OO}(r)$ at high T. Although the position of the first maximum of $C_Q(r)$ remains fixed for all the temperatures, the position of the second maximum moves slightly to the smaller r as the temperature decreases. A negative minimum at the fifth-neighbor distance $r \approx 0.32$ nm for high T implies that the local tetrahedral order parameters of a central molecule and its fifth neighbor are anticorrelated at $T > 250$ K. Interestingly, the anticorrelation at $r = 0.32$ nm changes to positive correlation below the $T_W \approx 250$ K.

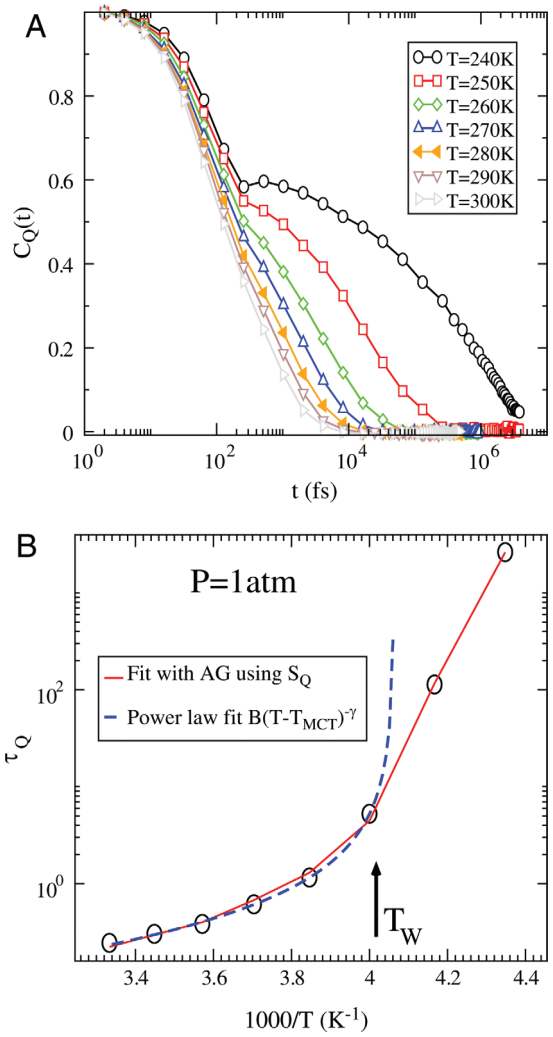

Fig. 3. Temperature dependence of time autocorrelation function of local tetrahedral order parameter and relaxation times. (*A*) Autocorrelation function $C_Q(t)$ of tetrahedral order parameter Q at various temperatures. $C_Q(t)$ is exponential at high temperatures but displays a visible two-step decay at low temperatures. (*B*) Correlation time τ_Q extracted from $C_Q(t)$ (circles). The solid line is the fit using the Adam–Gibbs relation (Eq. **13**) between the tetrahedral entropy $S_Q(T)$, and the tetrahedral relaxation time τ_Q. The dotted lines in *B* show the power-law fit $B(T - T_{MCT})^{-\gamma}$ with the fitting parameters $B = 25.39$, $T_{MCT} = 246.18$, and $\gamma = 1.17$. The behavior of τ_Q deviates from the power-law fit for the temperatures below the Widom-line temperature (indicated by a vertical arrow) T_W where a cross-over to Arrhenius behavior at lower temperature occurs.

$(1 - Q_k)^{3/2}\Delta Q_k$ because the number of independent dimensions is 5. We further assume that the order parameters of each molecule are independent, an assumption justified by the small value of $C_Q(r)$ (see Fig. 2*C*). Thus we can define the number of states $\Omega(Q_1, Q_2, \ldots, Q_N)$ in the interval between $(Q_1, Q_2, \ldots Q_N)$ and $(Q_1 + \Delta Q_1, Q_2 + \Delta Q_2, \ldots, Q_N + \Delta Q_N)$ as the product

$$\Omega(Q_1, Q_2, \ldots, Q_N) \equiv \Omega_0^N \prod_{k=1}^{N} \left[\frac{8}{3}(1 - Q_k)\right]^{\frac{3}{2}}, \qquad [10]$$

where $\Omega_0 = const$. Hence the tetrahedral entropy of the entire system is given by

$$S(Q_1, Q_2, \ldots, Q_N) \equiv NS_0 + \frac{3}{2}k_B \sum_{k=1}^{N} \ln(1 - Q_k), \qquad [11]$$

where k_B is the Boltzmann constant and $S_0 = k_B[\ln \Omega_0 + \frac{3}{2}\ln(\frac{8}{3})]$. If $P(Q, T)$ is the distribution of Q at a given temperature T, then the tetrahedral entropy $S_Q(T)$ per particle at temperature T can be written as

$$S_Q(T) \equiv S_0 + \frac{3}{2}k_B \int_{Q_{\min}}^{Q_{\max}} \ln(1 - Q)P(Q, T)dQ. \qquad [12]$$

In Fig. 4*A*, we show that $S_Q(T) - S_0$ decreases with decreasing temperature as expected.

We further define a measure of "tetrahedral specific heat" as $C_P^Q \equiv T(\partial S_Q(T)/\partial T)_P$. Fig. 4*B* shows the temperature dependence of C_P^Q and total specific heat C_P^{Total} for $P = 1$ atm. C_P^Q shows a maximum at $T \approx 250 \pm 10$ K $\approx T_W$, where the total specific heat C_P^{Total} also has a maximum (19, 31–33), suggesting that the fluctuations in tetrahedral order reach a maximum at $T_W(P)$. Moreover, comparing the tetrahedral specific heat in Fig. 4*B* with the total specific heat, we find that the C_P^Q is a major contribution to the C_P^{Total} and, particularly, the difference ΔC_P of the two specific heats remains a constant within the error bar for all temperatures studied, hence suggesting that C_P^Q is responsible for the Widom-line transformations.

To relate the tetrahedral entropy $S_Q(T)$ to the tetrahedral relaxation time $\tau_Q(T)$ associated with the local tetrahedral ordering,

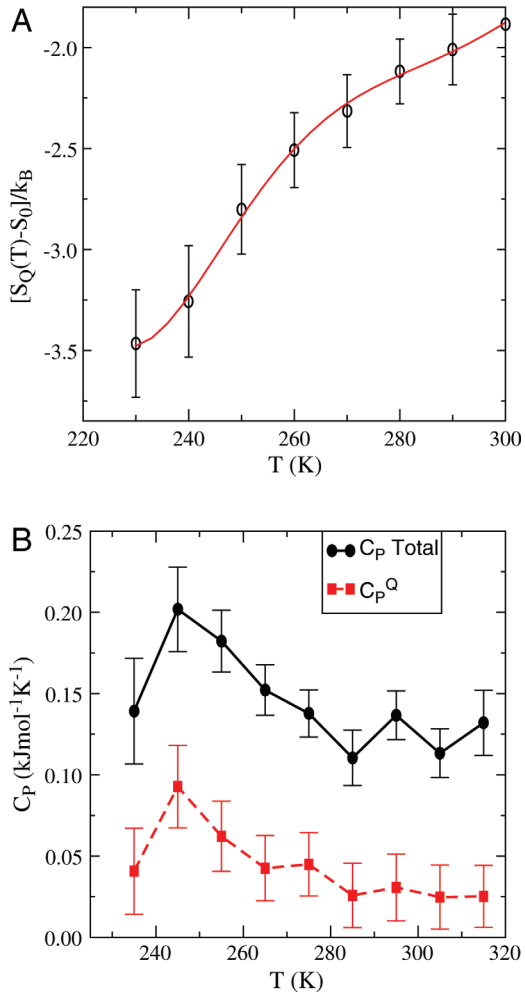

Fig. 4. Temperature dependence of tetrahedral entropy $S_Q(T)$ (*A*), defined in Eq. **11**, (the red solid line is a guide to the eye) and tetrahedral specific heat $C_P^Q = T(\partial S_Q/\partial T)_P$ (*B*), which has a maximum around the same temperature, $T \approx 250 \pm 10$ K $\approx T_W$, where the total specific heat C_P^{Total} has a maximum. Moreover, the difference ΔC_P of the two specific heats is a constant within the error bars for all the temperatures, hence suggesting that C_P^Q is responsible for the Widom-line transformations.

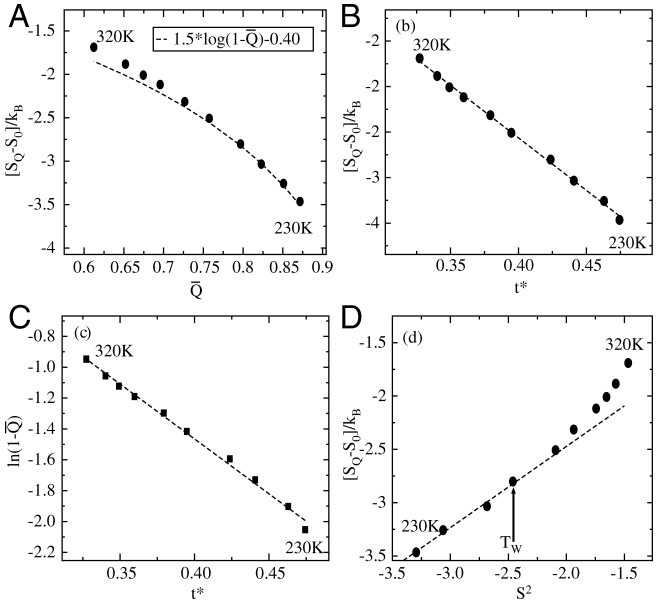

Fig. 5. Relation of tetrahedral entropy to tetrahedral order parameter and contribution of two-point translational correlations to entropy S^2 for temperatures $T = 230, 240, 245, 250, 260, 270, 280, 290, 300, 320$ K. (*A*) Test of the relation of Eq. **16** for the relation between the tetrahedral entropy S_Q and the tetrahedral order parameter $\bar{Q}$, assuming $F = -0.40$ independent of temperature. (*B*) S_Q as a function of t^* shows that S_Q decreases linearly with t^*. The dashed line is a linear fit through the data. (*C*) Fig. 5 *A* and *B* are consistent with the possibility that the average translational order parameter t^* varies as $\log(1-\bar{Q})$. (*D*) Dependence of S_Q on S_{ex}. S_Q changes linearly with S^2 at low temperatures, but the linearity begins to break down for $T > T_W \approx 250$ K.

we propose the following generalization of the Adam–Gibbs relation between the translational relaxation time and configurational entropy (39, 40),

$$\tau_Q(T) = \tau_Q(0)\exp[A/TS_Q(T)], \qquad [13]$$

where $\tau_Q(0)$ is the tetrahedral relaxation time at very large T, and A is a parameter playing the role of activation energy. Accordingly, we calculate $\tau_Q(T)$ (Fig. 3*B*) from $S_Q(T)$ by using Eq. **13** with three free parameters: A, $\tau(0)$, and S_0. We find that $S_0 \approx 4.21k_B$. The values of $\tau_Q(T)$ calculated by using Eq. **13** are within error bars of the values of $\tau_Q(T)$ calculated from the autocorrelation function (see Fig. 3*B*).

Fig. 3*B* is an Arrhenius plot of τ_Q, calculated from Eq. **13**. The temperature dependence of τ_Q is different at low and high temperatures, changing from non-Arrhenius (a T-dependent slope on the Arrhenius plot), which can be fit by a power law at high temperatures, to Arrhenius (a constant slope) at low temperatures (19, 20, 31–33).

Relation of Tetrahedral Entropy to Translational Order Parameter and Translational Entropy. In this section, we investigate the relation of S_Q with (*i*) the translational order parameter t^* (41) defined as

$$t^* \equiv \int |g(r) - 1|dr \qquad [14]$$

and (*ii*) the translational entropy S^2 (42, 43) obtained from the two-point translational correlations, which is defined as

$$S^2 \equiv -2\pi\rho k_B \int [g(r)log(g(r)) - (g(r) - 1)]r^2dr, \qquad [15]$$

where ρ is density and $g(r)$ is the oxygen–oxygen radial distribution function.

The excess entropy S^2 describes the contribution of two-point correlations to the total entropy of the system. It has been found that S^2 agrees very well with the total entropy in different systems including some models of water (43, 44).

In Fig. 5*A*, we show S_Q as a function of average tetrahedral order parameter $\bar{Q}$ for different temperatures and atmospheric pressure. S_Q varies approximately as $\log(1-\bar{Q})$ for the range of temperature studied. To justify this dependence of S_Q on $\bar{Q}$, we expand Eq. **12**,

$$S_Q(T) - S_0 = \frac{3}{2}k_B\left[\log(1-\bar{Q}) + F\right], \qquad [16]$$

where F is a function of moments of the fluctuations $(Q - \bar{Q})$. Hence, if we ignore F compared with the first term, then $S_Q \sim \log(1-\bar{Q})$. In Fig. 5*A*, we plot the above function (dashed line), assuming a constant $F = -0.40$ for all temperatures studied (230–320 K) and find that it agrees well with the values of S_Q computed by using Eq. **12** at low T but deviates slightly at high T.

Furthermore, Fig. 5*B* shows that S_Q varies linearly with t^*. Combining the results of Figs. 5 *A* and *B*, we form Fig. 5*C*, which demonstrates *s* simple relation between tetrahedral and translational oder parameters. We next find that, at low T, S_Q changes linearly with S^2; however it is nonlinear for high T. Note that a simple nonlinear relation between Q and t^* was found for the SPC/E model of water in the structurally anomalous region (13). Moreover, Fig. 5*D* shows that the temperature where this change in behavior occurs roughly coincides with the temperature of the Widom line T_W.

Discussion and Summary

In summary, we have studied the space and time correlations of local tetrahedral order Q, presumably related to local tetrahedral heterogeneities. We find that the space-dependent correlation of the the local tetrahedral order is anticorrelated for the molecules separated by 3.2 Å at high temperatures. This negative correlation changes to positive correlation upon decreasing T below the Widom temperature $T_W(P)$. Further, we define a measure of the tetrahedral entropy S_Q and find that the specific heat associated with the tetrahedral ordering is responsible for the Widom-line transformations. Finally, we find that S_Q well describes tetrahedral relaxation using the Adam–Gibbs relation. Moreover, we find a simple approximate relation between tetrahedral and translational order parameters $\bar{Q}$ and t^*. On the completion of this work, we were made aware by a referee that Lazardis and Karplus have studied the orientational entropy calculated from the two-point angular correlation function (45). Although they find that the orientational entropy of water has a major contribution to the total entropy, a contribution of orientational fluctuations to the total specific heat was not studied. The tetrahedral entropy $S(Q)$ defined in this paper captures the two-point orientational correlations but is much easier to compute in contrast to the computation of orientational entropy from the two-point angular correlation function and hence offers a rather simpler way to investigate the entropy associated with local structures.

ACKNOWLEDGMENTS. We thank J. R. Errington, P. H. Poole, S. Sastry, and F. W. Starr for fruitful discussions and the National Science Foundation Chemistry Division for support. P.K. acknowledges support from Keck Foundation National Academies Keck Futures Initiatives Award, and S.V.B. acknowledges partial support through the Dr. Bernard W. Gamson Computational Science Center at Yeshiva College.

1. Bernal JD, Fowler RH (1933) A theory of water and ionic solution, with particular reference to hydrogen and hydroxyl ions *J Chem Phys* 1:515–548.
2. Pople JA (1951) Molecular association in liquids. II. A theory of the structure of water *Proc R Soc London Ser A* 205:163–178.
3. Frank HS, Wen WY (1957) Structural aspects of ion-solvent interaction in aqueous solutions: A suggested picture of water structure *Discuss Faraday Soc* 24:133–140.
4. Eisenberg D, Kauzmann W (1969) *The Structure and Properties of Water* (Oxford Univ Press, New York).
5. Debenedetti PG (1997) *Metastable Liquids* (Princeton Univ Press, Princeton).
6. Soper AK, Phillips MG (1986) A new determination of the structure of water at 25-degrees-C. *Chem Phys* 107:47–60.

7. Sato H, Hirata F (1999) Ab initio study of water. II. Liquid structure, electronic and thermodynamic properties over a wide range of temperature and density. *J Chem Phys* 111:8545–8555.
8. Silvestrelli PL, Parrinello M (1999) Structural, electronic, and bonding properties of liquid water from first principles. *J Chem Phys* 111:3572–3580.
9. Tanaka H (1998) Fluctuation of local order and connectivity of water molecules in two phases of supercooled water. *Phys Rev Lett* 80:113–116.
10. Kusalik PG, Svishchev IM (1994) The spatial structure in liquid water. *Science* 265:1219–1221.
11. Steinhardt PJ, Nelson DR, Ronchetti M (1983) Bond-orientational order in liquids and glasses. *Phys Rev B* 28:784–805.
12. Chau P-L, Hardwick AJ (1998) A new order parameter for tetrahedral configurations. *Mol Phys* 93:511–518.
13. Errington JR, Debenedetti PG (2001) Relationship between structural order and the anomalies of liquid water. *Nature* 409:318–321.
14. Errington JR, Debenedetti PG, Torquato S (2002) Cooperative origin of low-density domains in liquid water. *Phys Rev Lett* 89:215503.
15. Yan Z, Buldyrev SV, Giovambattista N, Stanley HE (2005) Structural order for one-scale and two-scale potentials. *Phys Rev Lett* 95:130604.
16. Errington JR, Truskett TM, Mittal J (2006) Excess-entropy-based anomalies for a waterlike fluid. *J Chem Phys* 125:244502.
17. Yan Z, et al. (2007) Structure of the first- and second-neighbor shells of simulated water: Quantitative relation to translational and orientational order. *Phys Rev E* 76:051201.
18. Poole PH, Sciortino F, Essmann U, Stanley HE (1992) Phase behavior of metastable water. *Nature* 360:324–328.
19. Xu L, et al. (2005) Relation between the Widom line and the dynamic crossover in systems with a liquid-liquid critical point. *Proc Natl Acad Sci USA* 102:16558–16562.
20. Liu L, Chen SH, Faraone A, Yen CW, Mou CY (2005) Pressure dependence of fragile-to-strong transition and a possible second critical point in supercooled confined water. *Phys Rev Lett* 95:117802.
21. Mazza MG, Giovambattista N, Starr FW, Stanley HE (2006) Relation between rotational and translational dynamic heterogeneities in water. *Phys Rev Lett* 96: 057803.
22. Mazza MG, Giovambattista N, Stanley HE, Starr FW (2007) Connection of translational and rotational dynamical heterogeneities with the breakdown of the Stokes–Einstein and Stokes–Einstein–Debye relations in water. *Phys Rev E* 76:031203.
23. Sastry S, Angell CA (2003) Liquid–liquid phase transition in supercooled silicon. *Nat Mater* 2:739–743.
24. Morishita T (2006) How does tetrahedral structure grow in liquid silicon upon supercooling? *Phys Rev Lett* 97:165502.
25. Ganesh P, Widom M (2009) Liquid–liquid transition in supercooled silicon determined by first-principles simulation. *Phys Rev Lett* 102:075701.
26. Saika–Voivod I, Sciortino F, Poole PH (2000) Computer simulations of liquid silica: Equation of state and liquid–liquid phase transition. *Phys Rev E* 63:011202.
27. Katayama Y, et al. (2004) Macroscopic separation of dense fluid phase and liquid phase of phosphorus. *Science* 306:848–851.
28. Mahoney MW, Jorgensen WL (2000) A five-site model for liquid water and the reproduction of the density anomaly by rigid, nonpolarizable potential functions. *J Chem Phys* 112:8910–8922.
29. Yamada M, Mossa S, Stanley HE, Sciortino F (2002) Interplay between time–temperature-transformation and the liquid–liquid phase transition in water. *Phys Rev Lett* 88:195701.
30. Paschek D (2005) How the liquid–liquid transition affects hydrophobic hydration in deeply supercooled water. *Phys Rev Lett* 94:217802.
31. Kumar P, et al. (2007) Relation between the Widom line and the breakdown of the Stokes–Einstein relation in supercooled water. *Proc Natl Acad Sci USA* 104:9575–9579.
32. Kumar P (2006) Breakdown of the Stokes–Einstein relation in supercooled water. *Proc Natl Acad Sci USA* 103:12955–12956.
33. Kumar P, et al. (2006) Glass transition in biomolecules and the liquid–liquid critical point of water. *Phys Rev Lett* 97:177802.
34. Sciortino F, Geiger A, Stanley HE (1990) Isochoric differential scattering functions in liquid water: The fifth neighbor as a network defect. *Phys Rev Lett* 65:3452–3455.
35. Lee SL, Debenedetti PG, Errington JR (2005) A computational study of hydration, solution structure, and dynamics in dilute carbohydrate solutions. *J Chem Phys* 122:204511.
36. Gallo P, Sciortino F, Tartaglia T, Chen S-H (1996) Slow dynamics of water molecules in supercooled states. *Phys Rev Lett* 76:2730–2733.
37. Götze W (1999) Recent tests of the mode-coupling theory for glassy dynamics. *J Phys Condens Matter* 11:A1–A45.
38. Kumar P, Franzese G, Stanley HE (2008) Predictions of dynamic behavior under pressure for two scenarios to explain water anomalies. *Phys Rev Lett* 100:105701–105704.
39. Adam G, Gibbs JH (1965) On the temperature dependence of cooperative relaxation properties in glass-forming liquids. *J Chem Phys* 43:139–146.
40. Giovambattista N, Buldyrev SV, Starr FW, Stanley HE (2003) Connection between Adam–Gibbs theory and spatially heterogeneous dynamics. *Phys Rev Lett* 90:085506.
41. Yokoyama I (1999) On Dzugutov's scaling law for atomic diffusion in condensed matter. *Physica B* 269:244–248.
42. Truskett TM, Torquato S, Debenedetti PG (2000) Towards a quantification of disorder in materials: Distinguishing equilibrium and glassy sphere packings. *Phys Rev E* 62:993–1001.
43. Yan Z, Buldyrev SV, Stanley HE (2008) Relation of water anomalies to the excess entropy. *Phys Rev E* 78:051201.
44. Mittal J, Errington JR, Truskett TM (2006) Relationship between thermodynamics and dynamics of supercooled liquids. *J Chem Phys* 125:076102.
45. Lazaridis T, Karplus M (1996) Orientational correlations and entropy in liquid water. *J Chem Phys* 105:4294–4316.